ARTICLE

Amorphous Solid Water (ASW): Pulsed Laser Ablation of ASW/CO2 Thin Films

Oscar Rebolledo-Mayoral, Jaimie Stomberg, Stephanie McKean, H. Reisler,* and C. Wittig*

Department of Chemistry, University of Southern California, Los Angeles, California 90089, United States

ABSTRACT: Thin films composed of 400−500 monolayers (ML) of either amorphous solid water (ASW) or ASW/CO2 mixtures are grown atop a MgO(100) substrate under ultrahigh vacuum conditions. Samples are irradiated at an infrared frequency of 3424 cm^{-1}, which lies within the broad OH stretch band of condensed water. Ablation is achieved using 10 ns pulses whose energy (<2.7 mJ) is focused to a beam waist of approximately 0.5 mm. By using a time-of-flight mass spectrometer to monitor ablated material, excellent single-shot detection is demonstrated. This capability is essential because, in general, the first infrared pulse can induce irreversible changes throughout the irradiated volume. With ASW/CO2 samples, CO2 is released preferentially. This is not surprising in light of the metastability of the samples. Indeed, repeated irradiation of the same spot can rid the sample of essentially all of the CO2 in as little as a

few pulses, whereas only 10−20 ML of H2O are removed per pulse. The influence of the substrate is profound. It cools the sample efficiently because the characteristic time for heat transfer to the substrate is much less than the infrared pulse duration. This creates temperature gradients, thereby quenching processes such as explosive boiling (phase explosion) and the heterogeneous nucleation of cavities that take place at lower depths in significantly thicker samples, i.e., with sufficient inertial confinement. This efficient quenching accounts for the fact that only 10−20 ML of H2O are removed per pulse. The presence of small protonated water cluster ions in the mass spectra is interpreted as evidence for the trivial fragmentation mechanism examined assiduously by Lewis and co-workers. Mixed samples such as ASW/CO2, where species segregation plays a pivotal role, add interesting and potentially useful dimensions to the ablation phenomenon.
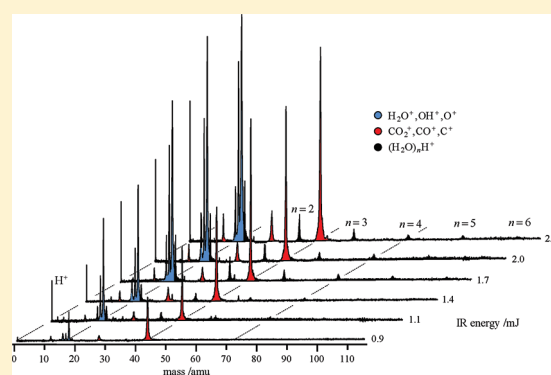
1. INTRODUCTION

Material ablation brought about through the application of pulsed electromagnetic radiation to condensed phase samples has found application in areas as diverse as medicine, materials growth and processing, cleaning, annealing, machining, analytical chemistry, nanoscience, and astrophysics.[1−3] In the work reported here, the ablation of thin films of amorphous solid water (ASW) and ASW/CO2 mixtures has been examined. This is relevant in astrophysics,[6−8] as well as the formation and disruption of clathrates. Though methane is the most important clathrate,[9] CO2 clathrate is germane to sequestration.[10] Recent research with ASW and ASW/CO2 has addressed the roles of sample morphology and its temperature variation, species segregation, and explosive boiling (phase explosion).[11−20]

Pulsed infrared radiation (10 ns duration, 3424 cm^{-1}) creates OH stretch excitation that converts to heat on a ps time scale.[4] Broad absorption spectra of ASW, crystalline ice, and liquid water ensure efficient excitation in samples whose character changes throughout the pulse. Moreover, (H2O)$_n$ clusters that enter the gas phase during the 10 ns pulse can absorb radiation from the same pulse that creates them. This is subtle, as absorption spectra differ with n in the small-n regime, say, $n \leq 6$.[5] These clusters cool only by fragmentation, as they are uncoupled from the substrate. The absorption depth (e^{-1}) for polycrystalline ice is ∼800 nm (at 3440 cm^{-1}),[21] which exceeds significantly the film

thicknesses used in the present study (typically ∼120 nm). Thus, energy deposition is rather uniform.

Theoretical models of laser-induced ablation that use molecular dynamics (MD) simulations have been put forward.[14,22−32] The groups of Garrison and Zhigilei have examined organic solids,[30−32] making seminal experimental and theoretical contributions. Likewise, theoretical studies of Lewis and co-workers[22,22,26,27,29] have provided a conceptual basis for judging experimental results. For example, Lorazo et al. examined strongly bound solids (silicon using 500 fs and 100 ps 266 nm pulses),[26,27] and Perez et al. examined molecular solids that have much larger absorption depths than silicon (4000 nm versus 5−10 nm, respectively) using ns pulses.[22] Despite the differences between the samples examined theoretically and those used here, the theoretical studies provide valuable insights.

In what follows, the experimental arrangement is described, with emphasis on the use of a high repetition rate (200 kHz) time-of-flight mass spectrometer (TOFMS). Single infrared pulse capability is demonstrated. This is important because the first pulse can induce irreversible change throughout the sample (a common observation in general in pulsed laser ablation). It is
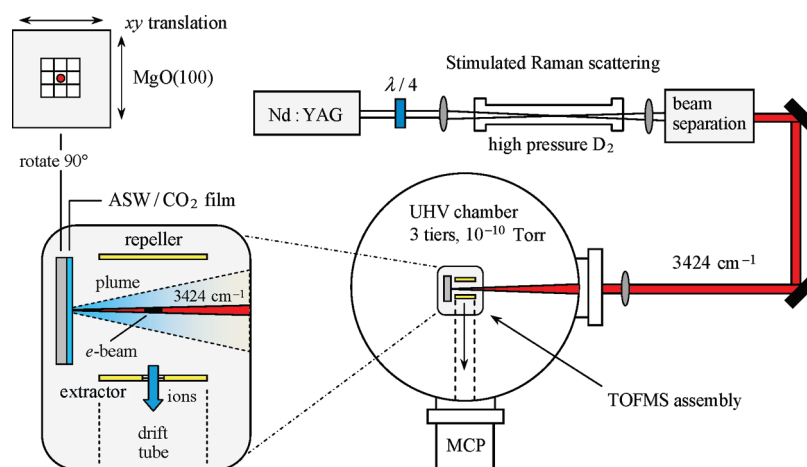
Figure 1. UHV chamber equipped with TOFMS, FTIR, Auger, and TPD. The TOFMS arrangement is indicated schematically. The second Stokes line $(3424\ cm^{-1})$ from stimulated Raman Scattering in high pressure D_2 gas excites the sample at normal incidence causing material to enter the gas phase. Ions are extracted at repetition rates up to 200 kHz. The black rectangle labeled e-beam indicates the portion of the ionized region that is extracted through the mesh aperture below it. Samples are irradiated in the nine areas indicated on the upper left to achieve signal averaging while maintaining single-pulse conditions.

shown that the preferential release of CO_2 can be pronounced and that species enter the gas phase in a sparse plume dominated by monomers and small water clusters, consistent with a trivial fragmentation mechanism.[25] Heat transfer to the MgO(100) substrate is estimated to take place in ~0.5 ns, resulting in pronounced temperature gradients. The amount of material removed with a single IR pulse is estimated to be 10−20 monolayers. This is more than an order of magnitude smaller than its counterpart from thicker films, other things being equal, in accord with efficient cooling by the substrate.[18,21] It is argued that this efficient cooling quenches phase explosion.

2. EXPERIMENTAL SECTION

The ablation of ASW and codeposited ASW/CO_2 films was examined using the arrangement indicated in Figure 1. Experiments were carried out in an ultrahigh vacuum (UHV) chamber $(10^{-10}$ Torr) using a pulsed (10 ns) $3424\ cm^{-1}$ radiation source and the high repetition rate TOFMS (Jordan TOF Products). The three-tier UHV chamber was described previously.[11,13,16] It is equipped for Fourier transform infrared (FTIR) spectroscopy, temperature programmed desorption (TPD),[11] and the laser-initiated ablation experiments reported herein.

A MgO(100) substrate was attached to a copper holder mounted on a LN_2-cooled coldfinger cryostat (McAllister Technical Services). MgO crystals (MTI Corporation) were cleaved on both sides in dry N_2 to expose (100) surfaces and transferred without delay into the vacuum chamber. Typical dimensions were 1 mm × 10 mm × 10 mm. After the chamber reached base pressure, the substrate was annealed to 600 K in oxygen to remove oxygen vacancies and contaminants.[11,33]

A surface holder that was used previously for FTIR and TPD experiments[13,16] was modified to reduce temperature gradients. The substrate was attached to a copper plate (14 mm × 10 mm × 0.3 mm) and secured by folding the edges of the plate over it. The $3424\ cm^{-1}$ radiation passed through a square opening (5 mm × 5 mm) in the plate. The surface holder was attached to one of two electrically isolated copper blocks on the coldfinger (Figure 2). The cryostat included *XYZ* translation and 360° rotation. Temperatures down to ~100 K were achieved with LN_2, and to ~90 K
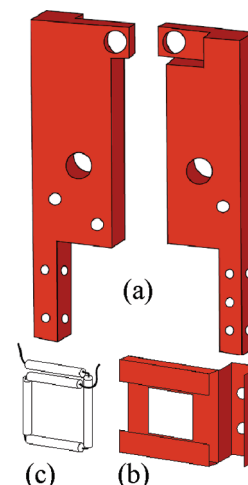

Figure 2. Exploded view of the substrate holder: (a) the electrically isolated copper blocks, (b) the folded copper plate that houses the substrate, and (c) the tantalum wire heater with ceramic sleeves, which is cemented to the back of the substrate holder. For resistive heating, the ends of the tantalum wires are connected to each of the electrically isolated blocks.

by bubbling helium through the LN_2. The sample was resistively heated using tantalum wire surrounded by ceramic sleeves cemented to the back of the copper plate with ceramic adhesive (Aremco 569). A chromel-alumel thermocouple was cemented to the substrate on the side opposite the copper block.

After the substrate was cooled to 90 K, ASW and ASW/CO_2 films were grown using background dosing. The dosing time was established using deposition rates determined by comparing the integrated TPD intensity of a water film with that of a water monolayer.[16] Optima LC/MS-grade water (Fisher Scientific) was degassed using freeze−pump−thaw cycles. H_2O and CO_2 (Gilmore Liquid Air, 99.99%) were introduced independently through precision leak valves. In this codeposition mode, CO_2 was embedded in the film during growth. Depending on substrate temperature, CO_2 sometimes aggregated atop the film. The film was annealed at 112 K and then cooled to 90 K to remove any CO_2 that might have accumulated atop the film.[13]

In the present experiments, H_2O/CO_2 ratios of 4:1 and 3:1 were used. These ratios are upper limits because some of the deposited CO_2 may re-enter the gas phase during deposition, and some of it finds its way to the surface and is removed at 112 K. We shall continue to refer to deposited samples using nomenclature such as 4:1 but with this caveat in mind. There is no reason to believe that the embedded CO_2 has a Poisson nearest-neighbor spacing distribution. It is likely that the deposited CO_2 is present to a significant extent in pockets following sample preparation. For example, if one considers the nearest-neighbor statistics for concentrations such as 25%, it is not possible to have a preponderance of CO_2 monomer.

Infrared radiation was generated by stimulated Raman Scattering (SRS) in D_2 ($\nu = 2987$ cm^{-1}) of the 1064 nm output of a Q-switched Nd:YAG laser (Continuum NY81C, 800 mJ, 10 ns) operating at 10 Hz. Circularly polarized radiation directed into a 1.1 m cell containing 60 atm of D_2 resulted in ~4% photon conversion efficiency for second Stokes radiation, S_2 (3424 cm^{-1}). To minimize gas degradation, laser energy fluctuations, and window damage in the Raman cell, the 1064 nm energy was limited to <185 mJ, resulting in a maximum S_2 energy of 2.7 mJ.[12] The laser and second Stokes energies were monitored using a calibrated pyroelectric meter (Ophir) and/or LN$_2$-cooled MCT detector (Cincinnati Electronics). Stokes lines were separated using a 60° CaF$_2$ prism. Only S_2 radiation entered the UHV chamber. The S_2 energy was attenuated with microscope slides. Prior to entering the chamber, the repetition rate was reduced to 1 Hz by using a chopper (ThorLabs MC1000). The S_2 radiation was focused with a 50 cm focal length CaF$_2$ lens to a diameter (1/e, near-Gaussian) of ~0.5 mm at the substrate.

Referring to Figure 1, the substrate was located such that the plume passed near the entry to the 0.5 m drift tube of the TOFMS. The incident infrared radiation was aligned such that its propagation vector was normal to the surface and perpendicular to the drift tube axis. The centermost region of the plume propagated through the center of the region between the repeller and extractor plates, where it was ionized with 70 eV electrons.

The smaller of the two electron-beam transverse dimensions (i.e., Figure 1, lower left, vertical dimension of the black rectangle) was approximately 1 mm at a distance of ~12 mm from the surface. The way extraction of individual ion packets works is as follows. To begin, the 70 eV electrons are deflected by the voltage difference between the repeller and extractor plates, which are held at 1800 and 1500 V, respectively. Consequently, species in the plume are not ionized. The extractor voltage is then switched to 1800 V, making it equal to the repeller voltage. This enables the 70 eV electrons to ionize species in the plume but without positive ions being extracted. After 2 μs, the extractor is switched back to 1500 V, and positive ions are extracted through a circular grid-aperture of 3 mm diameter. Extraction occurs immediately after the extractor voltage is switched to 1500 V. The cycle is then repeated. The resulting resolution achieved in our experiments is approximately $m/\Delta m = 130$. Ions were extracted at 100 kHz, i.e., mass spectra were recorded at 10 μs intervals. Signals persisted for as long as 300 μs after the laser firing.

To carry out a number of single-pulse experiments with the same film, the surface was moved such that a new region was irradiated with each laser firing (Figure 1, upper left). A distance of 1 mm between spots was sufficient to isolate results of different experiments on a single film. Deposited energy was rapidly transferred to the substrate. Note that ASW is a poor thermal conductor relative to crystalline MgO and the 14 crystalline forms of ice.[34] To prevent irradiation of the surface holder, the innermost 3 mm × 3 mm area was used. This allowed 9 experiments to be carried out with a single deposition.

Temporal profiles were recorded using a fast amplifier (SRS D-300 MHz) connected to an analog-to-digital converter (Gage CS 8500, 8 bit, 512k samples) with 2 ns resolution. Data processing and analyses were carried out using LabView programs (National Instruments) written for our experiments. Typically, single-pulse TOF spectra from the nine spots on the substrate are summed.

3. RESULTS

The interaction of infrared radiation with the amorphous thin film samples was studied under both single-pulse and multiple-pulse conditions. The IR frequency (3424 cm^{-1}) is slightly higher than the center of the broad absorption feature of the OH stretch fundamental in ASW.[13,16] It nonetheless lies well within the roughly 400 cm^{-1} full width at half-maximum (fwhm) of this feature. The results consist mainly of TOF mass spectra of the ejected plume of gaseous molecules and clusters following irradiation by single IR pulses. Irradiation using multiple pulses incident on the same spot underscores the virtue single-pulse capability.

Gas mixtures of H_2O and CO_2 codeposited at 90 K formed porous films.[13,16] As mentioned above, films were annealed to 112 K to remove surface-bound CO_2 and then cooled back to 90 K. Films of 400 and 500 monolayers (ML) were used in the present study. The IR radiation creates OH stretch excitation that is degraded to heat on a ps time scale.[4,35] Heat is transported to the substrate on a time scale that is much shorter than the laser pulse duration. Thus, material does not enter the gas phase for more than a few ns following cessation of the IR pulse.

Referring to Figure 3, each panel (20−240 μs) reflects the temporal evolution of the plume through a sequence of mass spectra recorded following a single laser firing. The signal at 10 μs is minuscule (not shown). The panels are normalized with respect to one another. Pronounced peaks are due to H_2O^+ ($m/e = 18$, black) and CO_2^+ ($m/e = 44$, red). Ions produced by the electron gun are extracted at a repetition rate of 100 kHz, i.e., each panel shows mass spectra separated by 10 μs intervals. For example, in Figure 3a, pulse 1, there are 22 individual mass spectra, each of which can be expanded to show its mass spectrum (vide infra Figure 5).

Columns a and b of Figure 3 show results for consecutive pulses incident on the same spot under different conditions. Pulse 1 in each series corresponds to the irradiation of an ASW/CO_2 mixture having the original composition and morphology. Subsequent pulses excite films that have been modified through previous irradiation. The data shown in panels a and b indicate that with 1.0 and 1.2 mJ, sufficient thermal energy is implanted to disrupt the ASW, allowing CO_2 to enter the gas phase. At these energies, water removal is less efficient for pulse 1. Referring to Figure 3c, no appreciable difference in its signal intensity was observed up to at least the first 10 pulses.

However, embedded CO_2 is depleted significantly within the first 4−5 pulses for energies ~1 mJ and as early as pulse 3 for 2.4 mJ (not shown). Figure 3a,b have initial H_2O/CO_2 concentration ratios of 4:1 and 3:1, respectively. Taking into account the higher ionization efficiency of CO_2 relative to H_2O and the fact that most of the H_2O signal (black) derives from the water monomer, we estimate that the amount of on-axis CO_2 in the

565

dx.doi.org/10.1021/jp203916m |*J. Phys. Chem. C* 2012, 116, 563–569
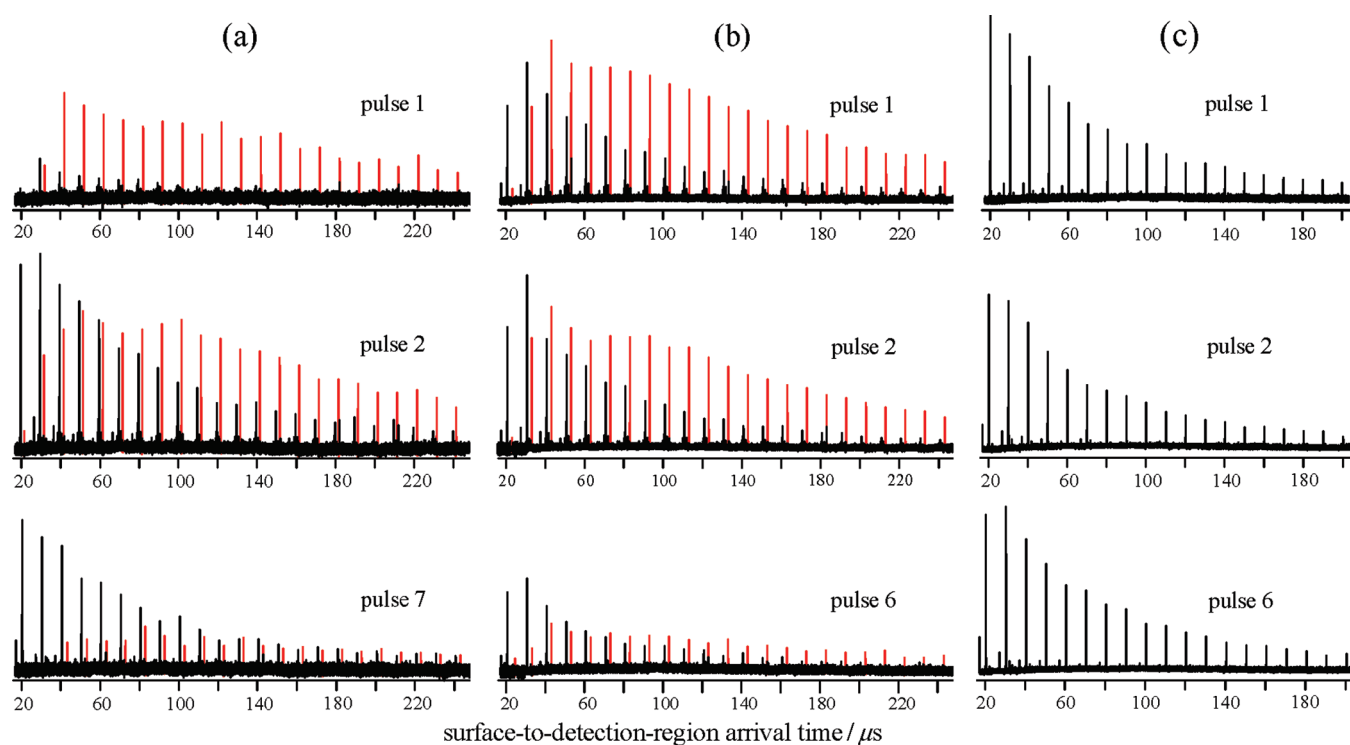
Figure 3. Horizontal axis is the arrival time at the detection region for material leaving the surface at $t = 0$. The TOFMS is operated at 100 kHz, i.e., individual spectra are recorded every 10 μs (Figures 4 and 5). (a) 500 ML (20% CO_2), 1.0 mJ: The first laser pulse liberates much more CO_2 (red) than H_2O (black). The second pulse liberates comparable amounts of CO_2 and H_2O. Pulse 7 liberates more H_2O than CO_2. Keep in mind that the H_2O/CO_2 ratio for deposited material is 4:1. (b) 400 ML (25% CO_2), 1.2 mJ: The same general trend as in panel a is observed, though less dramatic. (c) 400 ML of H_2O (no CO_2), 1.2 mJ. Signal at 10 μs is minuscule.

plume liberated after the first pulse is larger than that of H_2O by factors of roughly 7 and 2 in Figure 3a and b, respectively. For comparison, Figure 3c displays the evolution of the plume from a film containing no CO_2 following irradiation with 1.2 mJ.

Figure 3 shows that H_2O and CO_2 display different temporal profiles. In principle, such data can be analyzed to provide quantitative information about the velocity distributions of these species. However, this is not as easy as it might first appear; because detection efficiency increases for slow species, there is overlap between gas samples subjected to adjacent extractions, and the three-dimensional distributions of species in the plume must be determined, to say nothing of the usual enhancement of the noisy region by the Jacobian that transforms from time to energy. Consequently, this will be dealt with in a future publication.

To demonstrate the presence of clustered material in the plume following irradiation of ASW/CO_2 films, the IR energy was varied throughout the range 0.9–2.4 mJ. Figure 4 shows mass spectra obtained under single-pulse conditions but with signal averaging. To achieve signal averaging while maintaining single-shot conditions, the first three mass spectra recorded following a single pulse were summed. There is nothing special about the use of three; it is like three-point smoothing of a spectrum. This was carried out for each of the 9 spots (Figure 1, upper left), and data from the 9 spots were then summed. Thus, data from 27 mass spectra were averaged while maintaining single-pulse conditions.

Signals from protonated water clusters, $(H_2O)_nH^+$ with n up to 9 have been observed, as discussed later. Were material to enter the gas phase by evaporation at a well-defined temperature, it would result in monomers. The presence of clusters is in accord

with the trivial fragmentation mechanism discussed by Perez et al.[22] and Lewis et al.[25] Referring to Figure 4, signals due to H_2O monomer (blue), CO_2 (red), and H_2O-clusters (black) begin to appear at energies higher than ~0.9 mJ. At energies higher than 1.7 mJ, protonated water clusters are easily detected.

An expanded view of the H_2O cluster signals is shown in Figure 5, which displays results recorded after irradiating ASW/CO_2 mixtures with 2.4 mJ. Note that the H_2O^+ and CO_2^+ peaks are off-scale. Neutral[36] and even ionized[19] clusters have been observed previously under high infrared fluence conditions. Such experiments display a variety of cluster sizes with distributions that depend on irradiation conditions and detection methods. We looked for ionized clusters leaving the surface and found none. Throughout the period over which the data presented herein were recorded, we did not encounter serious problems with extraction-to-extraction fluctuations as long as the averaging described above (i.e., using 27 individual mass spectra) was carried out, notwithstanding the occasional rare burst of larger clusters, as described later.

4. DISCUSSION

Processes such as morphological change, phase transitions, transport, segregation, and heat flow in multicomponent molecular solids have been studied by a number of groups. Most theoretical studies have focused on strongly bound solids, though a number have addressed molecular solids,[14,30–32] including ASW and doped ASW films.[34,37–39] Given the long (10 ns) pulse duration in our experiments, it is not feasible to separate temporally the deposition of energy from consequent processes.
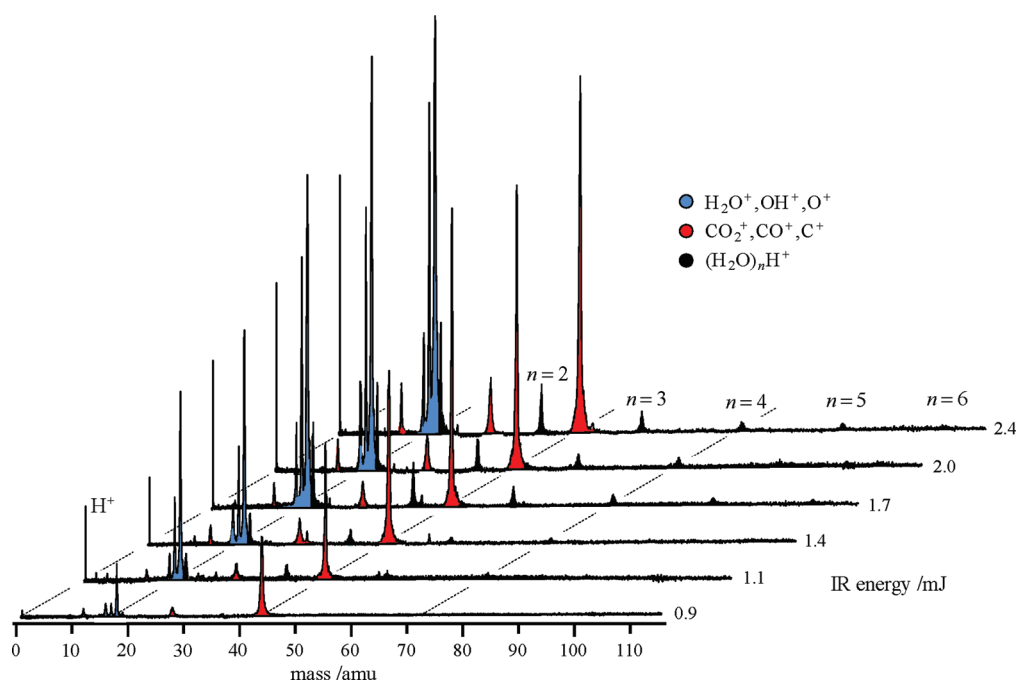
Figure 4. Mass spectra obtained under single-pulse conditions (400 ML, 25% CO_2) are presented for different IR energies. Peaks that derive from CO_2, monomer H_2O, and H_2O clusters are color-coded (red, blue, and black, respectively). Though some of the blue signal undoubtedly arises from H_2O clusters, these contributions are small. The single-pulse data shown here were obtained by summing contributions from the first three extractions (i.e., mass spectra) for each of the squares indicated in Figure 1.
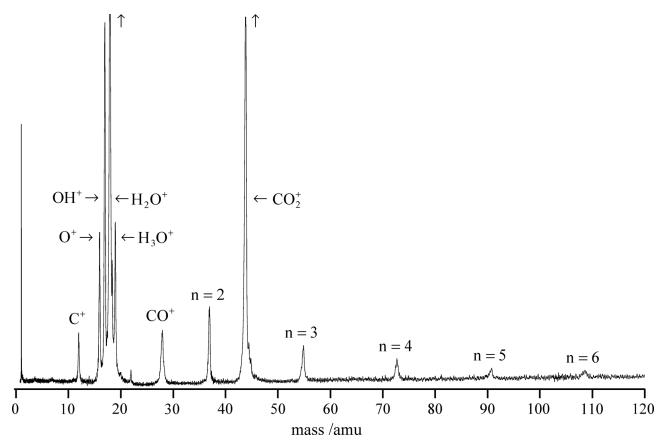

Figure 5. Spectrum highlighting the presence of protonated water cluster ions. Note that the H_2O^+ and CO_2^+ peaks are off-scale. Conditions: 400 ML (25% CO_2), 2.4 mJ, average of 9 spots, and 3 extractions for each spot.

Dynamical processes initiated by pulsed laser excitation have been studied theoretically by Lewis and co-workers.[22,26,27,29] Modeling silicon excited by 500 fs and 100 ps pulses (266 nm) has revealed ablation regimes.[27] The silicon samples are thicker than the ones used in the present study, in the sense that the distance over which radiation is absorbed is much smaller than the sample thickness, which is opposite our case. With 500 fs pulses, energy deposition precedes the dynamics. Topmost layers are ejected mainly as monomer and small clusters, whereas larger clusters emerge from lower depths. At the lowest depths, large voids appear, and a liquid shell of material is released,[27] in agreement with experimental observations of transient interference fringes following pulsed irradiation.[40,41] In the ns regime,

phase explosion is suppressed, though it can occur with sufficient inertial confinement.[22]

With thin ASW and ASW/CO_2 films, it is difficult to predict the rate of heat transfer to the substrate. Crystalline MgO has well-defined, high thermal conductivity, whereas the thermal conductivity of ASW is less than that of hexagonal and cubic ices.[34] The time required for heat to diffuse from the middle of the film to the substrate is $\tau_{\mathrm{diff}} = (d/2)^2/4D$, where D is the thermal diffusion coefficient, and d is the film thickness.[21] The 273 K value of D suggested by Livingston et al. yields $\tau_{\mathrm{diff}} \approx 500$ ps. On the basis of this crude estimate, we conclude that heat transfer occurs on a time scale that is short relative to the laser pulse duration. This results in a pronounced temperature gradient.

Clustered material in the plume has been interpreted as a signature of phase explosion.[8,22,24,27,36,42,43] Under the present conditions, though there may be some degree of explosive boiling, there is no reason to invoke phase explosion as an important mechanism. As the fluence is increased, irradiation of the topmost layers decomposes material entering the gas phase into smaller units. This pushes the transition region between small species (monomers plus small water clusters) and larger clustered species to lower depths. At the same time, efficient heat removal by the substrate quenches lower levels, thwarting the ejection of larger clusters.

Irradiation of the same spot continues to yield gas phase product, albeit with the composition of material entering the gas phase changing, i.e., the H_2O/CO_2 ratio increases. With the first few pulses, this change can be dramatic, as indicated in Figure 2a. Though often less dramatic, the propensity to emit, in the first few pulses, a larger percentage of CO_2 than the percentage of CO_2 present in the freshly prepared film is robust. This propensity has been observed in all of the experiments. In comparison, Livingston et al.[21] used comparable fluence, comparable photon energy, and longer pulse durations.
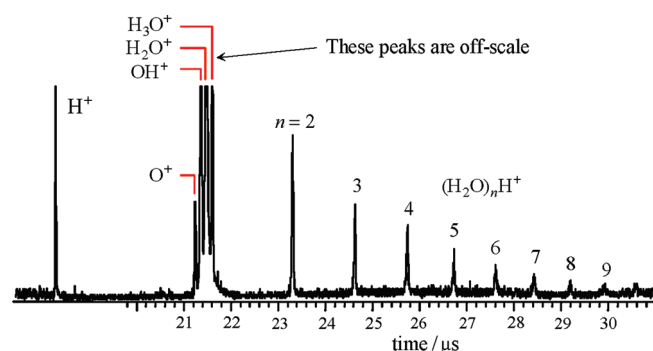
Figure 6. On rare occasion, relatively large cluster signals are observed, e.g., compare this spectrum to the one in Figure 5. The sample is 400 ML of ASW; IR energy is 1.7 mJ.

Their samples were typically one to two orders of magnitude thicker than ours, and the amount of material removed with a single pulse was ∼600 nm. This exceeds by a factor of several the sample thicknesses in our studies, and contrasts with the much smaller amount of material removed in our experiments, as discussed below. This difference is attributed to efficient cooling by the substrate.

Because the samples are metastable, initiating segregation is easy as it is energetically downhill. Whatever temperature rise accrues, and despite its spatial variation and transient nature, it promotes segregation. Metastable ASW/CO_2 gives way to more hydrogen bonding and CO_2 release. In Figure 3a, the majority of released material is CO_2, with relatively little H_2O despite the H_2O/CO_2 ratio of 4:1 in the deposited sample. This is extreme, but the propensity is present in all experiments. On rare occasion, signals from larger protonated ions were observed with ASW and ASW/CO_2 samples (Figure 6).

We do not know the size distribution of the neutral water clusters that give rise to the protonated water cluster ions. It is unlikely that if large neutral clusters were present they would not yield positive ions of comparable size. Also, in light of the efficient cooling brought about by the substrate, there is no reason to expect large clusters to be present in the plume.[14,25,27,31,36] Modeling studies using thicker samples and shorter excitation pulses indicate that large clusters are formed well below the surface, with small clusters emanating from closer to the surface.[27] In the present experiments, efficient cooling by the substrate inhibits the removal of H_2O from far below the surface.

A process that reduces cluster size is photoexcitation of clusters that enter the gas phase during a given infrared pulse and are exposed to the radiation for the remainder of the pulse. Suppose a cluster enters the gas phase within the first few ns of the 10 ns pulse. It is free to absorb photons for the remainder of the pulse. This will result in evaporation of H_2O molecules, causing the clusters to become smaller. This effect is convoluted with the blue shifts of the absorption spectra of clustered H_2O as the clusters get smaller. Consequently, laser-induced cluster shrinkage will slow because the absorption cross-section becomes too small. Namely, 3424 cm^{-1} lies on the high frequency side of the peak of the ASW absorption spectrum, whereas it lies on the low frequency side of the absorption spectra of small H_2O clusters.[5,21,44]

In the work reported here, the amount of material that enters the gas phase is small compared to the results reported in the theoretical studies. In the latter, material is entrained such that different species assume the same forward (plume) velocity.[14,30−32]

We observe no such entrainment. Referring to Figure 3, it is clear that CO_2 and H_2O each have different velocity distributions. There is insufficient density to support an expansion of the kind seen in the theoretical studies of Lorazo et al.[26,27]

It was noted earlier (Figure 3 and the surrounding discussion) that pulses of ∼1 mJ incident on ASW samples liberated approximately the same amount of H_2O per pulse for at least ten pulses. Therefore, because the sample consists of 400 ML of H_2O, less than 40 ML of H_2O is removed per pulse. If we examine further the respective amounts of on-axis CO_2 and H_2O, it is possible to obtain a smaller upper bound. The amount of deposited CO_2 is ∼100 ML in each of the ASW/CO_2 samples. Signals for CO_2 go to ∼0 before pulse number 10. If it is assumed that nearly all of the CO_2 is released through the application of successive pulses, the amount of H_2O released per pulse can be estimated. Specifically, by using the 70 eV cracking patterns and the ionization cross-sections, the amount of H_2O per pulse can be obtained. When this is carried out for columns a and b in Figure 3, it is found that 10−20 ML of H_2O is released into the gas phase with each pulse. The bottom line is that 10 ns pulses applied to samples of 400−500 ML remove only a small amount of water per pulse because of the efficient cooling provided by the substrate.

5. SUMMARY

Combining pulsed laser ablation with a high repetition rate (up to 200 kHz) time-of-flight mass spectrometer provides unique opportunities for studying thin films of ASW and doped ASW. Good S/N is achieved following irradiation with a single 3424 cm^{-1} pulse that excites the OH stretch vibration. This excitation is converted to heat on a ps time scale. Typically, individual TOF spectra spaced by 10 μs are recorded for >200 μs following single-pulse excitation. Single-pulse capability is essential, as the first pulse can alter the sample irreversibly. Change is apparent with ASW/CO_2, where the first pulse alters dramatically the composition. Signal averaging is achieved by translating the substrate laterally to ensure that a fresh sample is exposed to each pulse.

For ASW/CO_2 samples deposited in 3:1 and 4:1 ratios, the preferential release of CO_2 into the gas phase through the absorption of 3424 cm^{-1} radiation is not surprising considering the high degree of metastability of the samples. In an earlier study, it was shown that a modest amount of CO_2 remains embedded in the water host as the temperature is raised from 90 to 180 K at which point all of the water is removed.[13]

Small protonated water clusters are observed in the mass spectra. The size distribution of the neutral precursors is not known, though it is unlikely that significantly larger neutral clusters are involved. The presence of small clusters in the ejected plume is interpreted as evidence of the trivial fragmentation nature of the ablation.

Thin films atop an MgO(100) substrate are cooled efficiently. Consequently, some laser-induced processes that would transpire in thicker samples are quenched, e.g., phase explosion and fragmentation via the heterogeneous nucleation of voids.

■ AUTHOR INFORMATION

Corresponding Author
*E-mail: reisler@usc.edu (H.R.); wittig@usc.edu (C.W.).

■ ACKNOWLEDGMENT

568

dx.doi.org/10.1021/jp203916m |*J. Phys. Chem. C* 2012, 116, 563–569

■ REFERENCES

(1) *Laser Ablation and Desorption*; Miller, J. C., Haglund, R. F., Eds.; Academic Press: New York, 1998; Vol. 30.

(2) *Laser-Induced Breakdown Spectroscopy*, Singh, J. P., Thakur, S. N., Eds.; Elsevier: New York, 2007.

(3) Phipps, C. R. *Laser Ablation and Its Applications*; Springer: New York, 2007.

(4) Loparo, J. J.; Roberts, S. T.; Tokmakoff, A. *J. Chem. Phys.* **2006**, *125*, 194521.

(5) Paul, J. B.; Collier, C. P.; Saykally, R. J.; Scherer, J. J.; O'Keefe, A. *J. Phys. Chem. A* **1997**, *101*, 5211.

(6) Ehrenfreund, P.; Dartois, E.; Demyk, K.; d'Hendecourt, L. *Astron. Astrophys.* **1998**, *339*, L17.

(7) Ehrenfreund, P.; Kerkhof, O.; Schutte, W. A.; Boogert, A. C. A.; Gerakines, P. A.; Dartois, E.; d'Hendecourt, L.; Tielens, A. G. G. M.; van Dishoeck, E. F.; Whittet, D. C. B. *Astron. Astrophys.* **1999**, *350*, 240.

(8) Thrower, J. D.; Burke, D. J.; Collings, M. P.; Dawes, A.; Holtom, P. D.; Jamme, F.; Kendall, P.; Brown, W. A.; Clark, I. P.; Fraser, H. J.; McCoustra, M. R. S.; Mason, N. J.; Parker, A. W. *Astrophys. J.* **2008**, *673*, 1233.

(9) Sloan, E. D. *Nature* **2003**, *426*, 353.

(10) Dornan, P.; Alavi, S.; Woo, T. K. *J. Chem. Phys.* **2007**, *127*, 124510.

(11) Hawkins, S.; Kumi, G.; Malyk, S.; Reisler, H.; Wittig, C. *Chem. Phys. Lett.* **2005**, *404*, 19.

(12) Malyk, S. Transport and Guest-Host Interactions in Amorphous and Crystalline Ice. Ph.D. Thesis, University of Southern California, 2009.

(13) Malyk, S.; Kumi, G.; Reisler, H.; Wittig, C. *J. Phys. Chem. A* **2007**, *111*, 13365.

(14) Zhigilei, L. V. *Appl. Phys. A: Mater. Sci. Process.* **2003**, *76*, 339.

(15) Hodyss, R.; Johnson, P. V.; Orzechowska, G. E.; Goguen, J. D.; Kanik, I. *Icarus* **2008**, *194*, 836.

(16) Kumi, G.; Malyk, S.; Hawkins, S.; Reisler, H.; Wittig, C. *J. Phys. Chem. A* **2006**, *110*, 2097.

(17) Öberg, K. I.; Fayolle, E. C.; Cuppen, H. M.; van Dishoeck, E. F.; Linnartz, H. *Astron. Astrophys.* **2009**, *496*, 281.

(18) Livingston, F. E.; Smith, J. A.; George, S. M. *J. Phys. Chem. A* **2002**, *106*, 6309.

(19) Focsa, C.; Chazallon, B.; Destombes, J. L. *Surf. Sci.* **2003**, *528*, 189.

(20) Mihesan, C.; Ziskind, M.; Chazallon, B.; Therssen, E.; Desgroux, P.; Gurlui, S.; Focsa, C. *Appl. Surf. Sci.* **2006**, *253*, 1090.

(21) Livingston, F. E.; Smith, J. A.; George, S. M. *Anal. Chem.* **2000**, *72*, 5590.

(22) Perez, D.; Lewis, L. J.; Lorazo, P.; Meunier, M. *Appl. Phys. Lett.* **2006**, *89*, 141907.

(23) Bouilly, D.; Perez, D.; Lewis, L. J. *Phys. Rev. B* **2007**, *76*, 184119.

(24) Miotello, A.; Kelly, R. *Appl. Phys. A: Mater. Sci. Process.* **1999**, *69*, S67.

(25) Lewis, L. J.; Perez, D. *Appl. Surf. Sci.* **2009**, *255*, 5101.

(26) Lorazo, P.; Lewis, L. J.; Meunier, M. *Phys. Rev. Lett.* **2003**, *91*, 225502.

(27) Lorazo, P.; Lewis, L. J.; Meunier, M. *Phys. Rev. B: Condens. Matter Mater. Phys.* **2006**, *73*, 134108.

(28) Miotello, A.; Kelly, R. *Appl. Phys. Lett.* **1995**, *67*, 3535.

(29) Perez, D.; Béland, L. K.; Deryng, D.; Lewis, L. J.; Meunier, M. *Phys. Rev. B: Condens. Matter Mater. Phys.* **2008**, *77*, 014108.

(30) Zhigilei, L. V.; Garrison, B. J. *J. Appl. Phys.* **2000**, *88*, 1281.

(31) Zhigilei, L. V.; Kodali, P. B. S.; Garrison, B. J. *J. Phys. Chem. B* **1998**, *102*, 2845.

(32) Zhigilei, L. V.; Leveugle, E.; Garrison, B. J.; Yingling, Y. G.; Zeifman, M. I. *Chem. Rev.* **2003**, *103*, 321.

(33) Korolik, M.; Suchan, M. M.; Johnson, M. J.; Arnold, D. W.; Reisler, H.; Wittig, C. *Chem. Phys. Lett.* **2000**, *326*, 11.

(34) Johari, G. P.; Andersson, O. *Thermochim. Acta* **2007**, *461*, 14.

(35) Woutersen, S.; Emmerichs, U.; Nienhuys, H. K.; Bakker, H. J. *Phys. Rev. Lett.* **1998**, *81*, 1106.

(36) Mihesan, C.; Ziskind, M.; Chazallon, B.; Focsa, C.; Destombes, J. L. *Appl. Surf. Sci.* **2005**, *248*, 238.

(37) Andersson, O.; Suga, H. *Phys. Rev. B: Condens. Matter Mater. Phys.* **2002**, *65*, 140201.

(38) Slack, G. A. *Phys. Rev. B: Condens. Matter Mater. Phys.* **1980**, *22*, 3065.

(39) Wu, B. X. *J. Appl. Phys.* **2009**, *105*, 053502.

(40) Sokolowski-Tinten, K.; Bialkowski, J.; Cavalleri, A.; von der Linde, D.; Oparin, A.; Meyer-ter-Vehn, J.; Anisimov, S. I. *Phys. Rev. Lett.* **1998**, *81*, 224.

(41) Porneala, C.; Willis, D. A. *J. Phys. D: Appl. Phys.* **2009**, *42*, 155503.

(42) Martynyuk, M. M. *Combust. Explos. Shock Waves* **1977**, *13*, 178.

(43) Orlando, T. M.; Alkesandrov, A. B.; Herring, J. *J. Phys. Chem. B* **2003**, *107*, 9370.

(44) Cholette, F.; Zubkov, T.; Smith, R. S.; Dohnalek, Z.; Kay, B. D.; Ayotte, P. *J. Phys. Chem. B* **2009**, *113*, 4131.